ECOLOGY LETTERS

Ecology Letters, (2017) doi: 10.1111/ele.12870

LETTER

Eco-energetic consequences of evolutionary shifts in body size

Martino E. Malerba,*
Craig R. White and
Dustin J. Marshall

Centre of Geometric Biology, School of Biological Sciences, Monash University, Melbourne, Vic. 3800, Australia

**Correspondence: E-mail: martino.malerba@monash.edu*

Abstract

Size imposes physiological and ecological constraints upon all organisms. Theory abounds on how energy flux covaries with body size, yet causal links are often elusive. As a more direct way to assess the role of size, we used artificial selection to evolve the phytoplankton species *Dunaliella tertiolecta* towards smaller and larger body sizes. Within 100 generations (*c*. 1 year), we generated a fourfold difference in cell volume among selected lineages. Large-selected populations produced four times the energy than small-selected populations of equivalent total biovolume, but at the cost of much higher volume-specific respiration. These differences in energy utilisation between large (more productive) and small (more energy-efficient) individuals were used to successfully predict ecological performance (*r* and *K*) across novel resource regimes. We show that body size determines the performance of a species by mediating its net energy flux, with worrying implications for current trends in size reduction and for global carbon cycles.

Keywords

Allometry, artificial selection, evolutionary size shift, experimental evolution, geometric biology, metabolism, net energy flux, primary production, scaling.

Ecology Letters (2017)

INTRODUCTION

Size imposes fundamental physical and chemical constraints on individuals by mediating rates of energy utilisation (West *et al*. 2001, 2002; Brown *et al*. 2004). Specifically, increasing body mass usually decreases the mass-specific energy acquisition and use of a species (Brown *et al*. 2004). From an ecological prospective, body size influences competitive ability (Werner & Gilliam 1984), resource utilisation (De Roos & Persson 2013) and the ecological niche of a species (Bergmann 1847; Roff 1986). From an evolutionary prospective, virtually all life-history traits covary with body size (Peters 1983; Werner 1988; Reznick *et al*. 1990). For example, smaller species tend to grow faster (Savage *et al*. 2004) and have shorter life spans (Marba *et al*. 2007). As such, body size is perhaps the most fundamental trait in biology (De Roos *et al*. 2003).

The past 20 years have focused on the role of size in affecting the energy use of a species. A host of theories have been proposed for how size affects energy use, from bacteria to whales, with intense debate about the mechanistic drivers underlying broad-scale patterns (Brown *et al*. 2004; Anderson & Jetz 2005; Loeuille & Loreau 2006). Yet, for all the speculation about how size affects energy use, tests of how size influences energy acquisition are surprisingly rare (De Roos & Persson 2013). Of those studies that do examine the effect of size on energy acquisition, few tend to simultaneously account for energy use. It seems obvious that the productivity of an organism (via growth or reproduction) will depend on how size affects both energy acquisition and use – that is, the net energy flux. Yet, our understanding of size-dependent net energy flux remains surprisingly poorly resolved. This knowledge gap has taken on new significance given current trends in body size reduction across a range of taxa worldwide (Allendorf & Hard 2009).

Humans are driving species to smaller body sizes, both directly and indirectly, with unknown consequences (Allendorf & Hard 2009; Traill *et al*. 2014; Eikeset *et al*. 2016). Fishing and hunting are promoting the evolution of smaller body sizes, because larger individuals are targeted specifically and because higher mortality rates can select for earlier maturation at smaller sizes. For example, the heavily exploited fish species of Atlantic cod (*Gadus morhua*) has evolved to reproduce sooner and grow less, because fishing pressure dramatically decrease the chances of survival beyond a single round of reproduction (Olsen *et al*. 2004; Swain *et al*. 2007). Humans can also indirectly cause body size shifts via predator removal (Roy *et al*. 2003; Brodin & Johansson 2004; Preisser & Orrock 2012). Finally, global temperature increases are reducing body sizes, particularly of aquatic organisms (Daufresne *et al*. 2009; Gardner *et al*. 2011; Forster *et al*. 2012). In particular, phytoplankton species are decreasing in cell size in response to increasing temperatures (Atkinson *et al*. 2003; Daufresne *et al*. 2009; Polovina & Woodworth 2012). Phytoplankton fix around half the carbon on the planet (Field *et al*. 1998) but the consequences of size shifts for energy flows and global carbon cycles remain unknown. Overall, the cascading influences of changes in body size are poorly understood, but if body size affects the net energy flux of a species, these changes are likely to substantially alter the flow of energy through populations, communities and ecosystems.

Perhaps the most direct way to assess how size affects energy acquisition and usage is to engineer genetic differences in mean body size and evaluate its consequences for the net energy flux and fitness. We used artificial selection to generate differences in body size in the phytoplankton species *Dunaliella tertiolecta* (Chlorophyta) and measured traits at multiple times throughout the evolution of this species (i.e. generations 27, 70 and 103). We assessed different traits at multiple time points (rather than at the same generation) partly because

some of our hypotheses emerged from earlier tests, and also because some of our assays took days to perform, which meant that inevitably we could not conduct all of the assays at the same time point. We quantified how size shifts influenced the capacity of the evolved lineages to both acquire and use energy, as well as other ancillary traits. Then, we used these data to generate *a priori* predictions about vital ecological rates under different resource regimes. Finally, we tested these predictions by estimating key demographic rates across a resource gradient in later generations. We found that we can successfully predict the ecological dynamics of the evolved organisms based on size-dependent differences in energy acquisition and usage.

METHODS

Model species

The cosmopolitan, fast growing green alga *Dunaliella tertiolecta* (Butcher) was chosen as model species due to its intermediate cell size (relative to other phytoplankton species) and its capacity to grow well in laboratory conditions. Monoclonal batch cultures were sourced from the Australian National Algae Culture Collection (ANACC; strain code CS-14) and reared in standard F/2 algal media (without silica), prepared with 0.45 filtered seawater (Guillard 1975). All cultures used in the experiment were kept in a temperature-controlled room at 21 ± 2 °C with a 14–10 h day–night cycle at a light intensity of 150 μmol quanta m^{-2} s^{-1}. All cultures were handled aseptically with sterile material under a laminar-flow cabinet (Alternative Environmental Solutions fitted with high-efficiency particulate arresting filter, Australia Standards 4260, National Association of Testing Authorities certified).

Cell size evolution

Artificial selection on cell size was achieved through differential centrifugation. This method relies on larger cells sinking and forming a pellet at the bottom of a test tube at lower centrifugal forces compared to smaller cells, which instead will remain in the supernatant. On the 25th of April 2016, 72 independent 50 mL cultures were inoculated from the same mother culture into aseptic 75 cm^2 plastic cell culture flasks (Corning®, Canted Neck, Nonpyrogenic, Merck, Darmstadt, Germany): 30 lineages for large selection, 30 for small selection and 12 for control.

Selection for large cells was achieved by only retaining the biomass pellet after centrifuging (Eppendorf 5810, Hamburg, Germany) cultures at 38 × g (600 rpm) for 3 min. Conversely, small selection was achieved by retaining only the supernatant after centrifuging at 68 × g (800 rpm) for 4 min. At each selection round, centrifugation routines were carried out twice. At the end of the selection process, one more centrifugation at 239 × g (1500 rpm) for 4 min allowed replacing the supernatant with fresh media. Control cultures were not selected for: each control culture was diluted 5 times in fresh media, centrifuged at 239 × g (1500 rpm) for 4 min, and resuspended. Selection was repeated twice a week, on Mondays and Thursdays. Every Thursday, all cultures were moved to newly sterilised flasks.

Speed and duration of centrifugation routines were determined through pilot studies, to maximise selection differential while diluting biomass to approximately 20% of the initial density. Pilot studies on the selection differential protocol detected a symmetrical shift for both larger and smaller cells of 10% between cell size before and after selection. Furthermore, a preliminary analysis showed that centrifuging cultures for 5 min from 20 to 425 × g (500 to 2000 rpm) did not alter the growth rate of the species compared to samples that were not centrifuged ($F_{4,53} = 0.55$, $P = 0.7$). As cells started responding to selection throughout the experiment, centrifugation time and speed were gradually adjusted, to maintain a symmetric selection differential and comparable dilution rates.

Cell size determination

Mean cell volumes were analysed regularly every 3 generations for the first 12 generations, and every 15 generations thereafter. Mean cell volumes were calculated after measuring at least 200 cells with optical light microscopy from randomly selected lineages and after allowing three generations of neutral selection (i.e. without any centrifugation) before collecting photos. A 1 mL aliquot of culture was stained with Lugol's iodine at 2%. Photomicrographs were taken at 400× after loading 5 μL onto a slide gently covered with a cover slip. Cell area was calculated with ImageJ and Fiji (Schindelin *et al.* 2012) and cell biovolume was calculated assuming prolate spheroid shape, as recommended for this species by Sun & Liu (2003).

Staining cells with Lugol iodine solution can in some species lead to cell shrinkage (Montagnes *et al.* 1994). However, pilot studies showed no sign of shrinkage between samples of live cells and cells that were stained immediately ($F_{1,170} = 1.55$, $P = 0.21$) and between 0, 5 and 7 days after Lugol staining ($F_{1,128} = 0.97$, $P = 0.33$).

Experimental design and neutral selection

Phenotypic characterisation of the lineages started after 27 generations of size-selection, when a consistent difference between treatments emerged ($F_{2,69} = 23.47$, $P < 0.001$): at this stage, cell volumes were 10% larger in large-evolved lineages and 2% smaller in small-evolved cells, compared to control lineages (Fig. 1). Also, the mean density of single cells, calculated as cell weight divided by cell volume, did not differ among treatments (see Appendix S1). Prior to the assays, a 10 mL aliquot was sampled from each of the 72 evolving lineages (30 small, 30 large and 12 control) and fertilised with 40 mL autoclaved fresh media. To remove any environmental conditioning from selection protocols, experimental cultures were grown for three generations (a week) under neutral selection (i.e. with no centrifugation). Cells were maintained under nutrient-replete conditions during neutral selection, by adding new media 3 days before and the same day of the assays. All assays were carried out after standardising all lineages to the same blank-corrected optical density value of 0.27, a level of

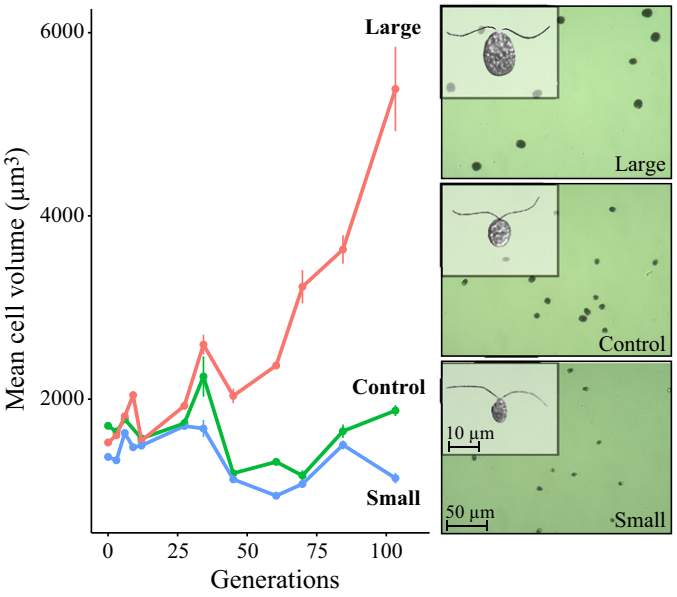

Figure 1 Effect of artificial selection on mean cell volume for size-selection treatments of small, control and large (±1SE). Net energy flux (Fig. 2a), chlorophyll concentration (Fig. 3a), sinking assays (Fig. 3b), swimming trials (Fig. 3c and d) and cell density (see Appendix S1) were measured at the 27th generation, while growth performance (Fig. 2c) at the 70th generation, and neutral selection assays (Appendix S3) at the 103th generation. Each point on the graph was calculated after measuring at least 200 cells from independent lineages. Photos on the right were taken with light microscopy after 103 generations: panoramic view of lugol-stained cells at 400X, and close-up of unstained single cells at 600X.

biomass that was tested to work well with all experimental protocols.

Dark and light metabolism

The rate of oxygen consumption (VO_2) was measured at 19 °C with 8 × 24-channel PreSens Sensor Dish Reader (SDR; AS-1 Scientific Wellington, New Zealand) with methods adopted from Malerba *et al.* (in press), White *et al.* (2011) and Warkentin *et al.* (2007). Before the experiment, all SDR were calibrated with air-saturated (AS) seawater (100% AS) and water containing 2% sodium sulphite (0% AS). After three generations of neutral selection, cultures were collected in exponential phase and placed in 5 mL sealed vials being careful to remove any air pocket from inside the vials. Biomass was standardised by optical density, a reasonable proxy for biovolume (see Appendix S2) but necessarily imposes different population densities, as at equal biomass smaller cells will be more abundant than larger cells – such a difference was unavoidable given our manipulation of size but we felt that it was more important to maintain constant biovolumes than densities. Pilot assays revealed that biovolume was a better predictor of resource usage by our cultures than population density, so all cultures were standardised by total biovolume before taking measurements. Sodium bicarbonate (2 mM) was added to the media to ensure photosynthesis and oxygen evolution were not limited by carbon availability. At least three blanks were filled with filtered supernatant and placed in each SDR. Then, the vials were placed horizontally under the light source, to avoid cell deposition on top of the oxygen sensor at the base of the vial. Samples were randomly allocated to the top two rows of the SDR, while blanks were placed in the bottom rows (pilot studies showed no row effect on blank measures). VO_2 measurements were taken at different light regimes (from 0 to 300 µmol quanta m^{-2} s^{-1} at increment of 50), randomising the order of light intensities and with dark periods separating each two light periods. At the end of the procedure, all measurements were repeated after swapping vials among the rows (yielding two sub-replicates per light level from which the mean was taken). At each light treatment, non-consumptive O_2 sensor spots monitored linear rates of change in O_2 saturation ($\dot{V}O2$; units µmol O_2 min^{-1}), calculated as:

$$\dot{V}O2 = \frac{m_a - \overline{m_b}}{100} V\beta 0_2 \quad (1)$$

where m_a is the rate of change of O_2 in each sample (% min^{-1}), $\overline{m_b}$ is the mean rate of O_2 change for all blanks of each plate (% min^{-1}), V is the water volume (0.005 L), and βO_2 is the oxygen capacity of air-saturated seawater at 20 °C and 35 ppt salinity (225 µmol O_2 L^{-1}). Per-cell $\dot{V}O2$ ($\dot{V}O2_{cell}$) was then calculated by dividing $\dot{V}O2$ by the total number of cells per µL in the vial, measured by flow cytometer (FlowCore, BD LSRII, BD Biosciences, San Jose, CA, USA) using CountBright absolute counting beads (Thermofisher, Waltham, MA, United States) as internal standards in each sample. Volume-standardised $\dot{V}O2$ ($\dot{V}O2_{vol}$) was calculated by dividing $\dot{V}O2_{cell}$ by the mean cell volume measured from each lineage. Finally, all $\dot{V}O2_{vol}$ rates were converted into calorific energy (J_{vol}), using the conversion of 512×10^{-3} J (µmol O_2)$^{-1}$ from Williams & Laurens (2010), assuming a macromolecular composition of 35% protein, 35% carbohydrates, 25% lipids and 5% nucleic acid.

The volume-standardised energy use of each lineage ($J_{vol,l}$) was analysed across light regimes as per Malerba *et al.* (in press), by fitting curves by Platt *et al.* (1980) of the form:

$$J_{vol,l} = P_{max,l}\left(1 - e^{-(\alpha(E-E_{c,l})/P_{max,l})}\right) \quad (2)$$

where l indicates each lineage, $P_{max,l}$ is the maximum potential volume-specific energy rate (units of J min^{-1} μm^{-3}), α_l is the initial slope of the curve (units of J min^{-1} μm^{-3} (µmol quanta s^{-1} m^{-2})$^{-1}$), and E and $E_{c,l}$ are the incident and compensation photon fluxes respectively (units µmol quanta s^{-1} m^{-2}). Models including an inhibition term were also fitted, but likelihood ratio test between the two nested models showed little support for a light inhibition coefficient in the data ($P > 0.05$).

Growth curves

Following three generations of neutral selection, time-series of optical density at 750 nm (as a proxy for total biovolume; see Appendix S2) were monitored from each lineage with microplate reader SPECTROstar® Nano (BMG labtech, Offenburg, Germany), after loading three independent 96-well plates with 250 µL of samples each (Corning® polystyrene, flat bottom, with lid, sterile, non-treated, Sigma-Aldrich). Each sample

was monitored daily (at the same time of the day) until reaching carrying capacity (7 days). Pilot studies showed that the daily evaporation within a well plate was very low (*c*. 1% per day) and was therefore not included in the analysis. Estimates for maximum exponential growth (r) and carrying capacity (K) were calculated for each lineage by fitting standard logistic growth models to daily time-series of optical density from three independent cultures with non-linear least squares techniques (function nls in *R*). Models that failed to converge or where residuals showed clear lack of fit were excluded from further analyses (i.e. 1 lineage for small and 2 for large, out of 72 lineages in total).

Additional assays

All lineages were also analysed for chlorophyll content, sinking rates, swimming speed and density of the cells. All assays followed standard methods (see figure legends for more details): volume-specific chlorophyll content (Fig. 3a), sinking rates (Fig. 3b), swimming performance (Fig. 3c and d) and mean density of a cell (see Appendix S1).

Statistical analysis

All analyses were carried out in R (R Core Team 2016). Non-linear logistic models were calibrated using package nlme with the function nls (Pinheiro *et al*. 2016; R Core Team 2016). Linear models were then used to assess the effects of the size-selection (i.e. small, control and large) on each variable of interest: population growth (parameters r and K), light and dark metabolism (parameters $P_{\max}$, E_c and α), cell density, chlorophyll content, swimming speed, swimming distance and sinking rate. Data transformations were employed whenever the residuals lacked normality. Also, in cases where treatments displayed unequal variances, treatment-specific variance coefficients were included in the model (varIdent function in R).

RESULTS

Cell size evolution

After 100 generations of selection there was a fourfold difference in cell volume between large-selected and small-selected lineages of *Dunaliella tertiolecta* (Fig. 1). We found that large-selected lines grew more than small-selected lines shrank, despite symmetrical artificial selection regimes (Fig. 1). Cell volume increased at a rate of 9.6% per 10 generations in large-selected cells ($F_{1,10} = 26.45$, $P < 0.001$), while it decreased at 5% per 10 generations in small-selected cells ($F_{1,10} = 20.31$, $P < 0.001$). Control cells were of intermediate sizes between small and large cells, without showing any trend in size over time ($F_{1,9} = 4.216$, $P = 0.07$).

Energy acquisition and usage

All of our measures of energy acquisition and usage are from samples at the 27th generation of size-selection and are here reported in volume-specific terms, so that large and small cells can be compared directly. Overall, large-selected cells were substantially more efficient at converting photons into energy, but also displayed higher rates of dark respiration (Fig. 2a). The maximum photosynthetic rate reached in large-selected cells was up to three times higher compared to small-selected and control cells ($P_{\max,l}$ in eqn 2; asymptote in Fig. 2a). Also, the rate of energy production was twice as high in large-selected cells compared to the other two treatments (α_l in eqn 2; initial slope in Fig. 2a). The compensation light intensity ($E_{c,l}$ in eqn 2; X-intercept in Fig. 2a) was lower in large compared to small and control cells, that is, large-selected cells needed less light to achieve 'break even' energy production. Finally, rates of dark respiration were twice as high in large cells compared to small and control cells (Y-intercept in Fig. 2a). The superior ability of large-evolved cells to produce energy at higher light conditions was consistent with their higher volume-standardised chlorophyll concentration (Fig. 3a). Later analysis on energy acquisition, energy usage and chlorophyll concentration of cells size-selected for more than 103 generations confirmed that the same qualitative differences detected at the 27th generation remained, mostly with differences among size treatments strengthening over time.

Predicting and testing productivity across environmental gradients

After measuring the net energy flux of size-selected cells at each light condition (Fig. 2a), we calculated the volume-specific daily net energy budget (i.e. photosynthesis during the day minus respiration at night) across a light gradient, varying in both light intensity and photoperiod (Fig. 2b). Under low energy conditions (i.e. low light intensities and/or short light durations), we predicted *a priori* that lower respiration costs of small-selected cells would lead to superior overall daily energy budgets compared to control and large cells (blue region in Fig. 2b). Conversely, we predicted that the higher photosynthetic capacities of large-selected cells would yield the highest productivity in high energy environments (i.e. high light intensities and/or extended light exposures; red region in Fig. 2b). These predictions were later confirmed empirically. When grown in low-light environments, small-selected cells showed faster exponential growth rates than control and large-selected cells (Fig. 2c). At intermediate lights, rates were statistically indistinguishable among size classes (Fig. 2c). Under high light regimes, large-selected cells displayed 77 and 45% faster exponential growth rates than small-selected and control cells respectively (Fig. 2c).

An unexpected finding was that small-selected cells achieved much lower total biovolumes at carrying capacity (Fig. 2c). We predicted that decreasing light intensity amplified the relative importance of lower maintenance costs of smaller organisms compared to greater energy capacity of larger organisms (Fig. 2a). But lower energy needs of smaller sizes came at a cost: smaller cells reached lower total biovolumes at carrying capacity (by as much as 40%), regardless of resource regimes (Fig. 2c).

Sinking rate and cell motility

Volume-standardised sinking rates did not show statistically significant differences among size-selected treatments

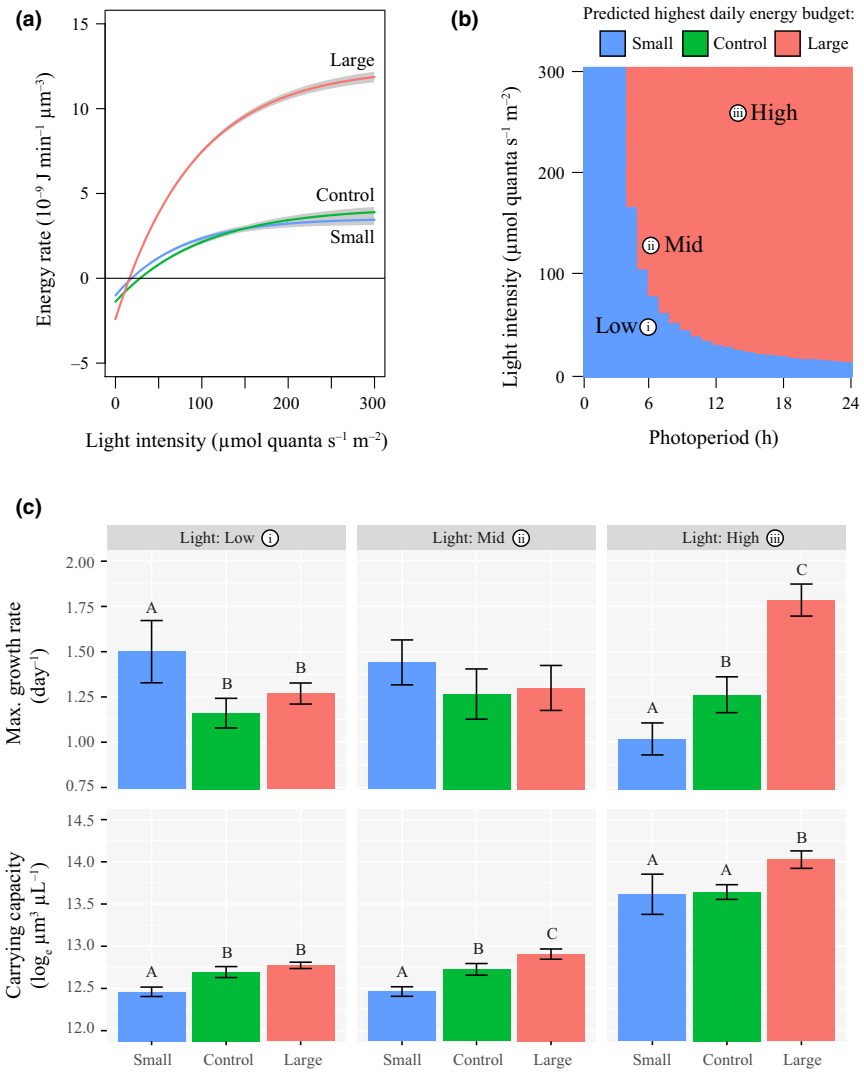

Figure 2 Energy analysis of size-selected lineages: first we measured the volume-specific net energy flux as a function of light intensity (a), then we predicted which size-evolved lineage would display the highest daily net energy budget across all combinations of light intensity and photoperiod (b), and finally we empirically tested these predictions at three light conditions (c). (a) P-I curve for the volume-specific net energy flux as a function of light intensity for each size-evolved treatment (± 95% confidence intervals). (b) Predicted highest daily energy budget estimated from mean rates of energy use (Fig. 2a) at all combinations of light:dark photoperiods and light intensities. Colours indicate the size-evolved treatment with the highest mean daily net energy budget. Indicated on the graph are the three light conditions used to empirically test these predictions: (i) low light (6:18 photoperiod at 50 µmol quanta s^{-1} m^{-2}), (ii) mid light (6:18 photoperiod at 120 µmol quanta s^{-1} m^{-2}), and (iii) high light (14:10 photoperiod at 250 µmol quanta s^{-1} m^{-2}). (c) Max. growth rates and carrying capacity measured at low, mid and high light conditions across size-evolved lineages (± 95% confidence intervals). Units of carrying capacity were converted to biovolume using linear calibration curves (see Appendix S2). Letters indicate significantly different groupings following Tukey's *post hoc* test.

($F_{2,34}$ = 2.86, P = 0.07; Fig. 3b). This was because smaller cells showed slower per-cell sinking rates ($F_{2,34}$ = 3.48, P = 0.04), but proportionally to their volume all treatments showed equal per-volume sinking rate. This result is consistent with comparable density of individual cells among size treatments (Fig. S1). Also, cells that were not size-selected showed higher (volume-standardised) swimming performances than small- and large-selected cells, with faster speeds (Fig. 3c) and for longer travelled distances (Fig. 3d).

DISCUSSION

Confronting *a-priori* predictions with empirical data is perhaps the most robust way to test a hypothesis. In this study, we first evolved cells towards smaller and larger sizes compared to the ancestral condition, estimated size-specific net energy production across size classes, and used these estimates to generate predictions about vital ecological rates across a resource gradient. Finally, we tested these predictions by measuring demographic rates across different resource conditions. Our results showed that we can successfully predict ecological dynamics solely based on the interplay between size-specific energy production, energy usage and resource availability. We found that larger sizes increased the volume-specific energy production of a cell by improving photosynthesis, but also increased volume-specific respiration rates in the dark. Consequently, larger cells showed faster population growth rates under higher resource regimes, but were inferior to smaller

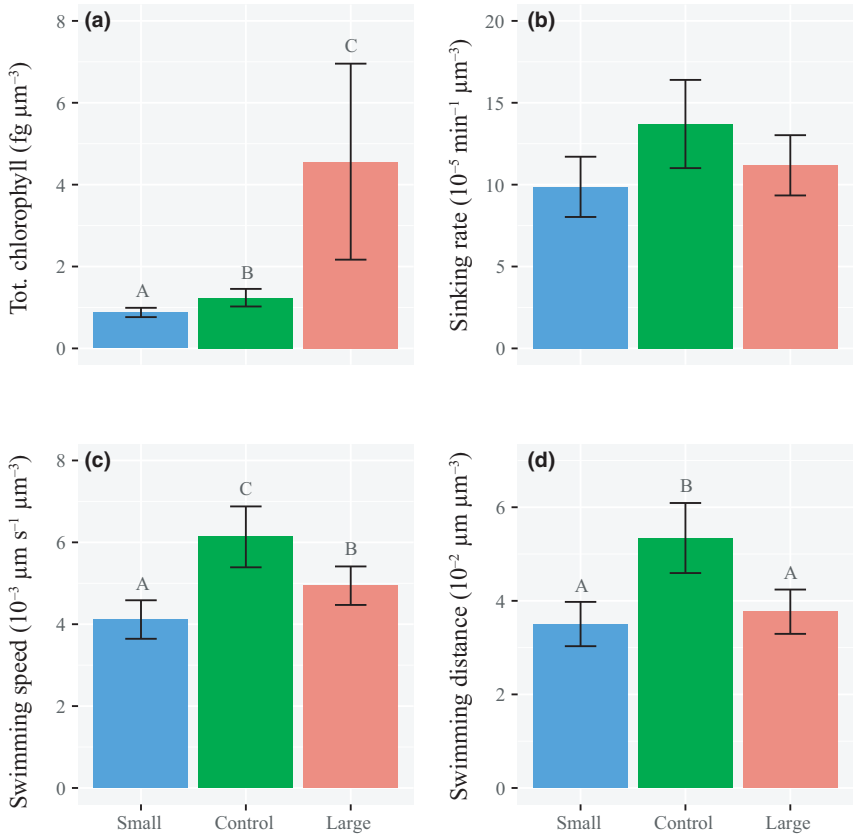

Figure 3 Volume-standardised mean traits (± 95% confidence intervals) among size-evolved treatments after 27 generations of size-selection for (a) total chlorophyll content (10^{-12} µg µm^{-3}), (b) sinking rate (min^{-1} µm^{-3}), (c) swimming speed (µm s^{-1} µm^{-3}) and (d) swimming distance (µm µm^{-3}). Letters indicate significantly different groupings following Tukey's *post hoc* test. (a) Vol-specific chlorophyll content was measured spectrophotometrically, as per Hiscox & Tsraelstam (1979). Briefly, a 1 mL aliquot from each lineage was resuspended in dimethyl suiphoxide (ACS reagent grade > 99.9%, Sigma-Aldrich), stored overnight at 4C, and total chlorophyll concentration of the sample was calculated as $0.0202 \times A_{645} + 0.00802 \times A_{663}$, where A_{645} and A_{663} are blank-corrected optical values at 645 and 663 nm. Total chlorophyll concentration was then divided by population density and by mean cell size. (b) Rates of cell sinking were calculated spectrophotometrically, using methods by Steele & Yentsch (1960). Cells were first immobilised by staining 2 mL of culture with 4% of formaldehyde solution (35 wt. % in H_20, Sigma-Aldrich). After an initial gentle resuspension, optical density (750 nm) was measured across a 3 mL cuvette every minute for 30 min, while keeping incubation temperature at 25 °C. As cells were sinking towards the bottom of the vial, the recorded absorbance decreased at a rate that is proportional to the mean sinking velocity of each particle. As optical densities decreased over time following a negative sinusoidal curve, decaying logistic curves described well the dynamics in the data. Negative r coefficients estimated by fitting logistic curves quantifies the mean sinking rates of the particles. We also tried alternative functional forms with fewer parameters (e.g. linear, negative exponential), but model selection with Akaike Information Criteria (Burnham & Anderson 2002) consistently favoured logistic functions. (c and d) Swimming speed and travelled distance were measured by analysing videos recorded under light microscopy at 100× magnification. A 20 µL aliquot for each lineage was loaded on a glass slide and covered with a 24 × 60 mm coverslip (LabServ®, Thermo Fisher). The setup was designed to allow enough water depth between the slide and the coverslip for cells to swim naturally in a 2D plane, while reducing any vertical movement. After waiting 2–5 min, 8 s footage was recorded for each lineage. Single-particle tracking was then performed in ImageJ and Fiji with TrackMate (Schindelin *et al.* 2012; Tinevez *et al.* 2016). Mean track statistics were then standardised by the mean cell size of the culture.

cells at lower resource regimes. However, larger cells consistently reached higher carrying capacities than smaller cells at all resource regimes – a discovery that is harder to explain. Other key traits, such as swimming speed and travelling distance, showed highest performance at control cells, perhaps because they maintained an optimal ratio of cell size to length of the swimming flagella. These results showed context-dependent costs and benefits of different cell sizes, which suggest natural limits on cell size evolution, and that current cell size is the product of conflicting selection pressures due to variable resource regimes in nature. Also, by imposing size-selective pressure on a common ancestor, we provided direct empirical evidence on the causal relationships between the body size of a species, and its energy flux and demographic rates. Finally, all assays were carried out after standardising cultures to the same total biovolume, as to also standardise for resource requirements among treatments. This standardisation necessarily confounds population densities (i.e. small-selected cultures have more cells), but in our system, biovolume drives dynamics more than the density of cells – population growth slows down more at equivalent biovolumes than at equivalent cell densities, indicating that total biovolume is a better predictor of total population resource requirements among size treatments.

Faster evolution towards larger sizes

Despite the application of symmetrical selection pressures for more than 100 generations of size-selection, cell volume increased two times faster in large-selected cells, than it decreased in small-selected cells. This trend of faster evolution towards larger sizes is opposite to studies on other organisms, which instead found mutational variance to be biased towards reducing sizes (Azevedo *et al*. 2002; Estes *et al*. 2005; Ostrow *et al*. 2007). We propose three (non-mutually exclusive) hypotheses to explain the higher success of evolving larger cells relatively to smaller cells. First, the fact that large cells performed better in high resource environments (i.e. 150 μmol quanta m^{-2} s^{-1} and 14:10 light cycle falls in red region of Fig. 2b) suggests our culturing conditions imposed a lower volume-specific daily net energy budget on smaller cells relative to larger cells. Thus, our experimental conditions inadvertently represented an additional selection pressure for increased size, conflicting with our selection regime towards smaller individuals. A second hypothesis is that faster evolutionary rates towards larger sizes may be due to larger developmental scope for increasing rather than decreasing cell volume. Many components within a cell are non-scalable and reducing the intracellular volume can potentially limit the overall functionality of a cell (Schmidt-Nielsen 1984; Maranon 2015). A third potential explanation for why cells evolved more towards larger sizes is that our methods to select for small cells favoured both smaller cells at mature stage and also younger cells at earlier ontogenetic stages. This latter group of cells will still have the potential to grow into larger cells, reducing the ultimate selection differential towards smaller sizes. Although a complete test of these hypotheses would require replicating the evolutionary experiment under different culture conditions (i.e. test if low light conditions induce faster evolution towards smaller sizes instead of larger) and with different selection protocols, we performed a preliminary test in which we analysed the rates of body size evolution after stopping artificial selection for size (see Appendix S3). Large-selected cells reared under relaxed artificial selection maintained their larger size only when exposed to high light levels, whereas low light regimes led to shrinkage of both large-selected and control cells (Appendix S3). These results support the first hypothesis that faster rates towards evolving larger sizes are due to a superior daily net energy budget. However, small-selected cells did not decrease their mean cell volume after being exposed to low light levels (Appendix S3), which also supports the second hypothesis of a lower boundary to cell size evolution.

Size evolution across resources

Our results provided direct empirical evidence for the importance of body size and resource levels in mediating the net energy assimilation of an organism. Pioneering studies have established that the productivity of a species can either increase (e.g. Sanderson *et al*. 1999) or decrease (e.g. Massie *et al*. 2010) with organismal body size (ontogenetic asymmetry; De Roos *et al*. 2013; Persson & de Roos 2013). Our results expand these findings, as they showed that the energy efficiency and productivity of an organism not only changed with its size but also with resource level (see also Ghedini *et al*. in press; Malerba *et al*. in press). Specifically, high light regimes disproportionately favoured the greater capacity of larger cells to create energy, while low light conditions benefited the lower maintenance costs of smaller cells. In nature, there are many examples where resource levels affect the size-structure of a population, by favouring the survival of either smaller or larger individuals: fish (Edeline *et al*. 2016), amphibian (Asquith & Vonesh 2012), colonial invertebrates (Ellison & Harvell 1989), molluscs (Smalley 1983), insects (Amarillo-Suarez *et al*. 2011) and plants (Bertrand *et al*. 2011). Here, we argue that the consequences of size reduction will also heavily depend on resource levels. If these same mechanisms were to be confirmed among other species, new assessments should be undertaken to evaluate the magnitude of the impacts that anthropogenic activities have on natural populations by increasing (e.g. nutrient eutrophication) or decreasing (e.g. habitat degradation) resource levels.

Size and temperature

Our results have interesting applicability to the widely observed negative covariance between body size and temperature (Daufresne *et al*. 2009; Gardner *et al*. 2011). Here, we showed that increasing cell size led to higher daily variation in energy use, by increasing both volume-specific rates of photosynthesis and respiration. At warmer temperatures, a smaller body size confers a fitness advantage in many uni- and multicellular organisms (Forster *et al*. 2011, 2013). Higher temperatures increase metabolic rates (Gillooly *et al*. 2001) and reducing body size might represent a strategy to limit fluctuations in energy budget between energy acquisition and energy utilisation. Large cells may simply be unable to store up sufficient energy during the day to make it through a dark, hot night. Alternatively, a reduction in body size at higher temperatures might be due to respiration being more temperature sensitive than energy acquisition processes. This latter hypothesis is supported by studies on both autotrophic and heterotrophic species (Coles & Jokiel 1977; Atkinson *et al*. 2003; Liang *et al*. 2013). In this case, the costs of larger body sizes increased more than the benefits.

Size and global carbon cycles

Our results have worrying implications for the impacts of global change on carbon fixation in the ocean. We find that simple intuitions about populations of identical biomass but different body sizes do not hold. For example, we calculated that a large cell of 5000 μm^3 in volume can produce up to four times more energy than the combined production of five small cells of 1000 μm^3 each. If increased temperatures select for smaller cell sizes, as seems likely (Peter & Sommer 2012), then our results suggest that these cells will become nutrient limited at much lower resource levels, decreasing productivity by as much as 40%.

In addition to rising temperatures, our findings suggest that also resource limitation can act as an additional selective pressure towards reduction in organismal size. Decreasing

resources amplified the relative importance of lower maintenance costs of smaller organisms compared to greater energy capacity of larger organisms. But the lower energy needs of smaller sizes came at a cost: here, we showed that smaller sizes reached much lower total biovolumes at carrying capacity, regardless of resource regimes. This may be because smaller organisms tend to have lower C:N or C:P ratios and can therefore produce less biovolume than larger organisms from the same limiting resources (Maranon *et al*. 2013; Maranon 2015). If these same relationships were to be confirmed for other species, future global warming scenarios will select for smaller organisms not just by increasing temperatures but also by reducing available resources. This represents an unanticipated 'one-two punch' for aquatic primary productivity – decreasing both production and carrying capacity under lower resource regimes. Climate change is predicted to increase ocean stratification, which will reduce the transfer of nutrients to the surface and limit primary productivity in the euphotic zone. Aquatic primary producers are responsible for nearly half of the biospheric net photosynthesis (Field *et al*. 1998), and an additional reduction in autotrophic biomass could act as a positive feedback by reducing the ocean ability to mitigate anthropogenic carbon emissions.

ACKNOWLEDGEMENTS

We thank Prof Andrew Hirst, the editor, and two anonymous reviewers for helpful comments on this manuscript. Also, we thank Lucy Chapman, Dr. Maria del Mar Palacios Otero, Dr. Liz Morris, Dr Marcelo Lagos Orostica, Belinda Comerford, Annie Guillaume, Tim Landells and the Monash Micro-Imaging Centre for their help with laboratory procedures. We also acknowledge Prof John Beardall, Dr Michael McDonald, Prof Emilio Marañón, Prof Sean R. Connolly, Prof Kirsten Heimann, Prof David Grasham, Prof Anastasios Melis and Dr Florian Berner for insightful suggestions. We would like to express our gratitude to Ricardo San Martin, Stewart Crowley and John Arvanitakis for logistical support at Monash University. Finally, we are particularly grateful to the Australian Research Council for financial support (grants DP0987626, DP110101776, FT130101493 to C. R. White, and DP110103529 to D. J. Marshall). The authors declare no conflict of interest.

AUTHORSHIP

All authors contributed to designing the study. MEM conducted the experiment and collected the data. MEM and DJM carried out statistical analyses. MEM wrote the initial draft of the manuscript, while DJM and CRW provided substantial feedback. All authors gave final approval for publication.

DATA ACCESSIBILITY

All data and codes generated in this study are available in Dryad (https://doi.org/10.5061/dryad.bc1gb). Also in the file are photos taken with light microscopy showing the different cell sizes among size-selected lineages.

REFERENCES

Allendorf, F.W. & Hard, J.J. (2009). Human-induced evolution caused by unnatural selection through harvest of wild animals. *Proc. Natl Acad. Sci. USA*, 106, 9987–9994.

Amarillo-Suarez, A.R., Stillwell, R.C. & Fox, C.W. (2011). Natural selection on body size is mediated by multiple interacting factors: a comparison of beetle populations varying naturally and experimentally in body size. *Ecol. Evol*., 1, 1–14.

Anderson, K.J. & Jetz, W. (2005). The broad-scale ecology of energy expenditure of endotherms. *Ecol. Lett*., 8, 310–318.

Asquith, C.M. & Vonesh, J.R. (2012). Effects of size and size structure on predation and inter-cohort competition in red-eyed treefrog tadpoles. *Oecologia*, 170, 629–639.

Atkinson, D., Ciotti, B.J. & Montagnes, D.J. (2003). Protists decrease in size linearly with temperature: ca. 2.5% degrees C(-1). *Proc. Biol. Sci*., 270, 2605–2611.

Azevedo, R.B., Keightley, P.D., Lauren-Maatta, C., Vassilieva, L.L., Lynch, M. & Leroi, A.M. (2002). Spontaneous mutational variation for body size in Caenorhabditis elegans. *Genetics*, 162, 755–765.

Bergmann, C. (1847). Ueber die Verhältnisse der Wärmeökonomie der Thiere zu ihrer Grösse (Concerning the relationship of heat conservation of animals to their size). *Gottinger Studien*, 3, 595–708.

Bertrand, R., Gegout, J.-C. & Bontemps, J.-D. (2011). Niches of temperate tree species converge towards nutrient-richer conditions over ontogeny. *Oikos*, 120, 1479–1488.

Brodin, T. & Johansson, F. (2004). Conflicting selection pressures on the growth/predation risk trade-off in a damselfly. *Ecology*, 85, 2927–2932.

Brown, J.H., Gillooly, J.F., Allen, A.P., Savage, V.M. & West, G.B. (2004). Toward a metabolic theory of ecology. *Ecology*, 85, 1771–1781.

Burnham, K.P. & Anderson, D.R. (2002). *Model selection and multimodel inference: a practical information-theoretic approach*, 2nd edn. Springer-Verlag, New York.

Coles, S.L. & Jokiel, P.L. (1977). Effects of temperature on photosynthesis and respiration in hermatypic corals. *Mar. Biol*., 43, 209–216.

Daufresne, M., Lengfellner, K. & Sommer, U. (2009). Global warming benefits the small in aquatic ecosystems. *Proc. Natl Acad. Sci. USA*, 106, 12788–12793.

De Roos, A.M. & Persson, L. (2013). *Population and Community Ecology of Ontogenetic Development*. Princeton Press, Princeton, NJ.

De Roos, A.M., Persson, L. & Mccauley, E. (2003). The influence of size-dependent life-history traits on the structure and dynamics of populations and communities. *Ecol. Lett*., 6, 473–487.

De Roos, A.M., Metz, J.A. & Persson, L. (2013). Ontogenetic symmetry and asymmetry in energetics. *J. Math. Biol*., 66, 889–914.

Edeline, E., Terao, O. & Naruse, K. (2016). Empirical evidence for competition-driven semelparity in wild medaka. *Popul. Ecol*., 58, 371–383.

Eikeset, A.M., Dunlop, E.S., Heino, M., Storvik, G., Stenseth, N.C. & Dieckmann, U. (2016). Roles of density-dependent growth and life history evolution in accounting for fisheries-induced trait changes. *Proc. Natl Acad. Sci. USA*, 113, 15030–15035.

Ellison, A.M. & Harvell, C.D. (1989). Size hierarchies in Membranipora membranacea: do colonial animals follow the same rules as plants? *Oikos*, 55, 349–355.

Estes, S., Ajie, B.C., Lynch, M. & Phillips, P.C. (2005). Spontaneous mutational correlations for life-history, morphological and behavioral characters in Caenorhabditis elegans. *Genetics*, 170, 645–653.

Field, C.B., Behrenfeld, M.J., Randerson, J.T. & Falkowski, P. (1998). Primary production of the biosphere: integrating terrestrial and oceanic components. *Science*, 281, 237–240.

Forster, J., Hirst, A.G. & Atkinson, D. (2011). How do organisms change size with changing temperature? The importance of reproductive method and ontogenetic timing. *Funct. Ecol*., 25, 1024–1031.

Forster, J., Hirst, A.G. & Atkinson, D. (2012). Warming-induced reductions in body size are greater in aquatic than terrestrial species. *Proc. Natl Acad. Sci. USA*, 109, 19310–19314.

Forster, J., Hirst, A.G. & Esteban, G.F. (2013). Achieving temperature-size changes in a unicellular organism. *ISME J*., 7, 28–36.

Gardner, J.L., Peters, A., Kearney, M.R., Joseph, L. & Heinsohn, R. (2011). Declining body size: a third universal response to warming? *Trends Ecol. Evol*., 26, 285–291.

Ghedini, G., White, C.R. & Marshall, D.J. (in press). Does energy flux predict density-dependence? An empirical field test. *Ecology*, doi:10.1002/ecy.2033

Gillooly, J.F., Brown, J.H., West, G.B., Savage, V.M. & Charnov, E.L. (2001). Effects of size and temperature on metabolic rate. *Science*, 293, 2248–2251.

Guillard, R.R.L. (1975). Culture of phytoplankton for feeding marine invertebrates. In: *Culture of Marine Invertebrate Animals* (eds Smith, W.L., Chanley, M.H.). Plenum Press, New York, pp. 26–60.

Hiscox, J.D. & Tsraelstam, G.F. (1979). A method for the extraction of chlorophyll from leaf tissue without maceration. *Can. J. Bot*., 57, 1332–1334.

Liang, J., Xia, J., Liu, L. & Wan, S. (2013). Global patterns of the responses of leaf-level photosynthesis and respiration in terrestrial plants to experimental warming. *J. Plant Ecol*., 6, 437–447.

Loeuille, N. & Loreau, M. (2006). Evolution of body size in food webs: does the energetic equivalence rule hold? *Ecol. Lett*., 9, 171–178.

Malerba, M.E., White, C.R. & Marshall, D.J. (in press). Phytoplankton size-scaling of net-energy flux across light and biomass gradients. *Ecology*, doi: 10.1002/ecy.2032.

Maranon, E. (2015). Cell size as a key determinant of phytoplankton metabolism and community structure. *Ann. Rev. Mar. Sci*., 7, 241–264.

Maranon, E., Cermeno, P., Lopez-Sandoval, D.C., Rodriguez-Ramos, T., Sobrino, C., Huete-Ortega, M. *et al*. (2013). Unimodal size scaling of phytoplankton growth and the size dependence of nutrient uptake and use. *Ecol. Lett*., 16, 371–379.

Marba, N., Duarte, C.M. & Agusti, S. (2007). Allometric scaling of plant life history. *Proc. Natl Acad. Sci. USA*, 104, 15777–15780.

Massie, T.M., Blasius, B., Weithoff, G., Gaedke, U. & Fussmann, G.F. (2010). Cycles, phase synchronization, and entrainment in single-species phytoplankton populations. *Proc. Natl Acad. Sci. USA*, 107, 4236–4241.

Montagnes, D.J.S., Berges, J.A., Harrison, P.J. & Taylor, F.J.R. (1994). Estimating carbon, nitrogen, protein, and chlorophyll a from volume in marine phytoplankton. *Limnol. Oceanogr*., 39, 1044–1060.

Olsen, E.M., Heino, M., Lilly, G.R., Morgan, M.J., Brattey, J., Ernande, B. *et al*. (2004). Maturation trends indicative of rapid evolution preceded the collapse of northern cod. *Nature*, 428, 932–935.

Ostrow, D., Phillips, N., Avalos, A., Blanton, D., Boggs, A., Keller, T. *et al*. (2007). Mutational bias for body size in rhabditid nematodes. *Genetics*, 176, 1653–1661.

Persson, L. & de Roos, A.M. (2013). Symmetry breaking in ecological systems through different energy efficiencies of juveniles and adults. *Ecology*, 94, 1487–1498.

Peter, K.H. & Sommer, U. (2012). Phytoplankton cell size: intra- and interspecific effects of warming and grazing. *PLoS ONE*, 7, e49632.

Peters, R.H. (1983). *The Ecological Implications of Body Size*. Cambridge University Press, Cambridge, UK.

Pinheiro, J., Bates, D., DebRoy, S. & Sarkar, D. & R Core Team (2016). nlme: Linear and Nonlinear Mixed Effects Models. R package version 3.1-128, http://cran.r-project.org/package = nlme. Last accessed 17 September 2017.

Platt, T., Gallegos, C.L. & Harrison, W.G. (1980). Photoinhibition of Photosynthesis in Natural Assemblages of Marine-Phytoplankton. *J. Mar. Res*., 38, 687–701.

Polovina, J.J. & Woodworth, P.A. (2012). Declines in phytoplankton cell size in the subtropical oceans estimated from satellite remotely-sensed temperature and chlorophyll, 1998–2007. *Deep Sea Res. Part II*, 77, 82–88.

Preisser, E.L. & Orrock, J.L. (2012). The allometry of fear: interspecific relationships between body size and response to predation risk. *Ecosphere*, 3, 1–27.

R Core Team (2016). R: A language and environment for statistical computing. R Foundation for Statistical Computing, Vienna, Austria. http://www.r-project.org/. Last accessed 17 September 2017.

Reznick, D.A., Bryga, H. & Endler, J.A. (1990). Experimentally induced life-history evolution in a natural population. *Nature*, 346, 357–359.

Roff, D.A. (1986). Predicting body size with life history models. *Bioscience*, 36, 316–323.

Roy, K., Collins, A.G., Becker, B.J., Begovic, E. & Engle, J.M. (2003). Anthropogenic impacts and historical decline in body size of rocky intertidal gastropods in southern California. *Ecol. Lett*., 6, 205–211.

Sanderson, B.L., Hrabik, T.R., Magnuson, J.J. & Post, D.M. (1999). Cyclic dynamics of a yellow perch (Perca flavescens) population in an oligotrophic lake: evidence for the role of intraspecific interactions. *Can. J. Fish Aquat. Sci*., 56, 1534–1542.

Savage, V.M., Gilloly, J.F., Brown, J.H. & Charnov, E.L. (2004). Effects of body size and temperature on population growth. *Am. Nat*., 163, 429–441.

Schindelin, J., Arganda-Carreras, I., Frise, E., Kaynig, V., Longair, M., Pietzsch, T. *et al*. (2012). Fiji: an open-source platform for biological-image analysis. *Nat. Methods*, 9, 676–682.

Schmidt-Nielsen, K.N.U.T. (1984). The limits on evolution of body size. In: *Size, Function, and Life History* (ed. Calder, WA). Courier Corporation, North Chelmsford, MA, p. 431.

Smalley, T.L. (1983). Possible effects of intraspecific competition on the population structure of a solitary vermetid mollusk. *Mar. Ecol. Prog. Ser*., 14, 139–144.

Steele, J.H. & Yentsch, C.S. (1960). The Vertical Distribution of Chlorophyll. *J. Mar. Biol. Assoc. U.K*., 39, 217–226.

Sun, J. & Liu, D.Y. (2003). Geometric models for calculating cell biovolume and surface area for phytoplankton. *J. Plankton Res*., 25, 1331–1346.

Swain, D.P., Sinclair, A.F. & Mark Hanson, J. (2007). Evolutionary response to size-selective mortality in an exploited fish population. *Proc. Biol. Sci*., 274, 1015–1022.

Tinevez, J.Y., Perry, N., Schindelin, J., Hoopes, G.M., Reynolds, G.D., Laplantine, E. *et al*. (2016). TrackMate: an open and extensible platform for single-particle tracking. *Methods* 115, 80–90

Traill, L., Schindler, S. & Coulson, T. (2014). Demography, not inheritance, drives phenotypic change in hunted bighorn sheep. *PNAS*, 111, 13223–13228.

Warkentin, M., Freese, H.M., Karsten, U. & Schumann, R. (2007). New and fast method to quantify respiration rates of bacterial and plankton communities in freshwater ecosystems by using optical oxygen sensor spots. *Appl. Environ. Microbiol*., 73, 6722–6729.

Werner, E.E. (1988). Size, scaling, and the evolution of complex life cycles. In *Size-Structured Populations: ecology and Evolution* (eds Ebenman, B., Persson, L.). Springer, Berlin Heidelberg Berlin, Heidelberg, pp. 60–81.

Werner, E.E. & Gilliam, J.F. (1984). The ontogenetic niche and species interactions in size structured populations. *Annu. Rev. Ecol. Syst*., 15, 393–425.

West, G.B., Brown, J.H. & Enquist, B.J. (2001). A general model for ontogenetic growth. *Nature*, 413, 628–631.

West, G.B., Enquist, B.J. & Brown, J.H. (2002). Ontogenetic growth: modelling universality and scaling reply. *Nature*, 420, 626–627.

White, C.R., Kearney, M.R., Matthews, P.G., Kooijman, S.A. & Marshall, D.J. (2011). A manipulative test of competing theories for metabolic scaling. *Am. Nat*., 178, 746–754.

Williams, P.J.L.B. & Laurens, L.M. (2010). Microalgae as biodiesel & biomass feedstocks: review & analysis of the biochemistry, energetics & economics. *Energy & Environmental Science*, 3, 554–590.

SUPPORTING INFORMATION

Additional Supporting Information may be found online in the supporting information tab for this article.

Editor, Stephan Munch
Manuscript received 3 August 2017
First decision made 14 September 2017
Manuscript accepted 30 September 2017